ECCOMAS Congress 2016
VII European Congress on Computational Methods in Applied Sciences and Engineering
M. Papadrakakis, V. Papadopoulos, G. Stefanou, V. Plevris (eds.)
Crete Island, Greece, 5–10 June 2016

DYNAMIC ANALYSIS OF SPECIAL CARS ON UNEVEN ROADS

Szymon Tengler

Department of Mechanics, University of Bielsko-Biala,
Willowa 2, 43-309 Bielsko-Biala, Poland
e-mail: stengler@ath.bielsko.pl

Keywords: dynamics analysis, special cars, uneven road surface; contact point.

Abstract. *The method of the dynamic analysis of special cars with a high gravity centre is presented in this article. The method proposed by the authors includes a comprehensive mathematical model of the car, and this model is supplemented with the models of uneven road surface, algorithms to determine the contact point between the tire and the road surface, and programs to perform computer simulations. In the article the mathematical model of the cooperation between road surface and tires are discussed in details. As it is known the road acts on the tire in a form of the reaction forces which should be applied in the concrete point named "contact point C". Thus, it is very important to determine this point location correctly. For this purpose the special mathematical models of the road surface and the algorithms to define the contact point location are developed. Two mathematical models of the road are discussed – continuous and discrete one. Two algorithms to find the location of the contact point are presented, as well. According to the conception of the authors names of the algorithms refer to the essence of the matter of the procedures assumed. The first of them – named Plane – can be used considering the continuous model of the surface, and the second – named 4Points – in the case of the discrete model of this surface.*

1 INTRODUCTION

While designing special cars with a high gravity centre (Figure 1), which move along the uneven road surface and are prone to a loss of stability (e.g. rollover), an essential issue is to take a preparation phase into account and to investigate a mathematical model of a constructed car.

Figure 1 Technical rescue vehicle of fire service as an example of a special vehicle with a high gravity centre

While considering motion of these type of cars on uneven road surface an important issue is to determine cooperation between road surface and tires. In this case a mathematical road surface model and also special algorithms for determine a location of contact point are needed.

Computer simulations of a motion of this model, performed in a case of different variants of constraints, can predict a lot of potential threats, and the conclusions drawn from them can constitute important guidelines for car designers. It is important for the prepared mathematical model of the car to be a sufficiently accurate representation of the real system. According to the car designers the computer simulations of an appropriately prepared mathematical model enable to shorten time of testing on a real prototype of the car, and also to reduce costs of the designing process.

2 MATHEMATICAL FORMALISM

For needs of the dynamics analysis, vehicles with high gravity centre can be modeled as multibody systems in a form of open kinematic chains. In this case the location (the position and orientation) of particular bodies should be know. Authors of the proposed method use joint coordinates basing on the approach applied in robotics. The proposed method is based on use of the homogenous transformation matrices with dimensions 4x4, which enable to make transformations between the assumed coordinate systems (related with bodies) [1].

If a position of any point A in the given coordinate system $\{j\}$, expressed by position vector ${}^{\{j\}}\mathbf{r}_A$ of dimensions 3x1, is known, then the position of this point in the coordinate system $\{i\}$ can be determined by the position vector ${}^{\{i\}}\mathbf{r}_A$ of dimensions 3x1 (Figure 2) using only one arithmetic operation, namely multiplication:

$$ {}^{\{i\}}\mathbf{r}_A^* = {}^{\{i\}}_{\{j\}}\mathbf{T}\,{}^{\{j\}}\mathbf{r}_A^* \tag{1} $$

where: ${}^{\{i\}}\mathbf{r}_A^* = \begin{bmatrix} {}^{\{i\}}\mathbf{r}_A \\ 1 \end{bmatrix}$, ${}^{\{j\}}\mathbf{r}_A^* = \begin{bmatrix} {}^{\{j\}}\mathbf{r}_A \\ 1 \end{bmatrix}$ - position vectors of dimensions 4x1, named vectors of homogenous coordinates, determining the position of point A in the system $\{i\}$ and $\{j\}$, respectively,

${}^{\{i\}}_{\{j\}}\mathbf{T} = \begin{bmatrix} {}^{\{i\}}_{\{j\}}\mathbf{R} & {}^{\{i\}}\mathbf{r}_j \\ 0 \quad 0 \quad 0 & 1 \end{bmatrix}$ – the transformation matrix of dimensions 4x4 from the coordinate system $\{j\}$ to the system $\{i\}$,

${}^{\{i\}}_{\{j\}}\mathbf{R} = \begin{bmatrix} \hat{X}_j \cdot \hat{X}_i & \hat{Y}_j \cdot \hat{X}_i & \hat{Z}_j \cdot \hat{X}_i \\ \hat{X}_j \cdot \hat{Y}_i & \hat{Y}_j \cdot \hat{Y}_i & \hat{Z}_j \cdot \hat{Y}_i \\ \hat{X}_j \cdot \hat{Z}_i & \hat{Y}_j \cdot \hat{Z}_i & \hat{Z}_j \cdot \hat{Z}_i \end{bmatrix}$ – the rotation matrix of dimensions 3x3 from the coordinate system $\{j\}$ to the system $\{i\}$ (elements of this matrix are dot products of the versors).

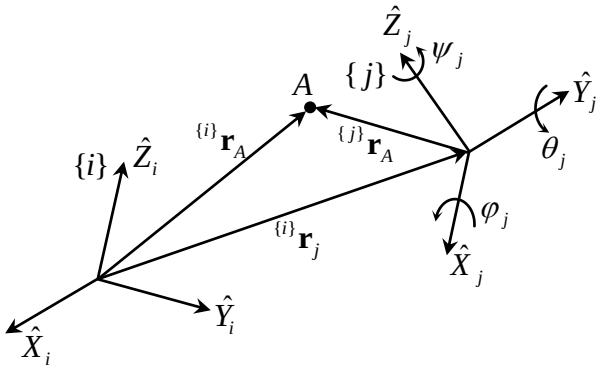

Figure 2. Determining the A point position in the coordinate system $\{i\}$ and $\{j\}$

3 MATHEMATICAL MODEL OF THE CAR

In the vehicle model, assumed in the form of open kinematic chain, 12 subsystems as rigid bodies were distinguished: frame, cabin, engine, car body, front and rear axle, two axle stubs, wheels connected by 6 spring-damper elements, respectively (Figure 3).

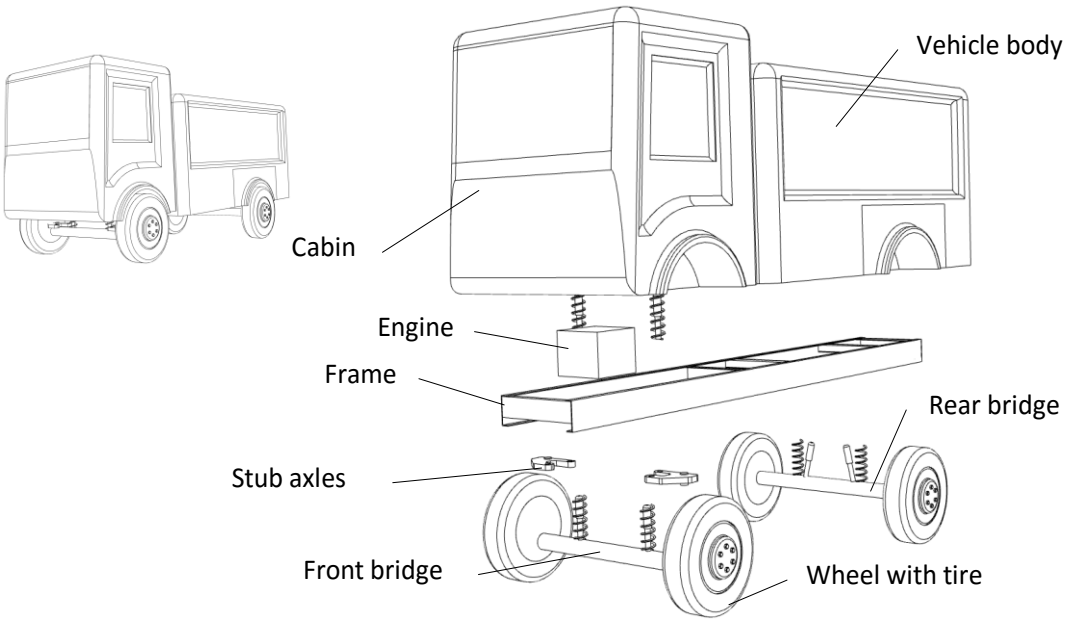

Figure 3 Components of the modelled car

The structure of the discussed chain can be considered as a tree structure, in which each body has a determined number of degrees of freedom (dof) in relation to the preceding body (see Figure 4). The vehicle model in question has 19 degrees of freedom.

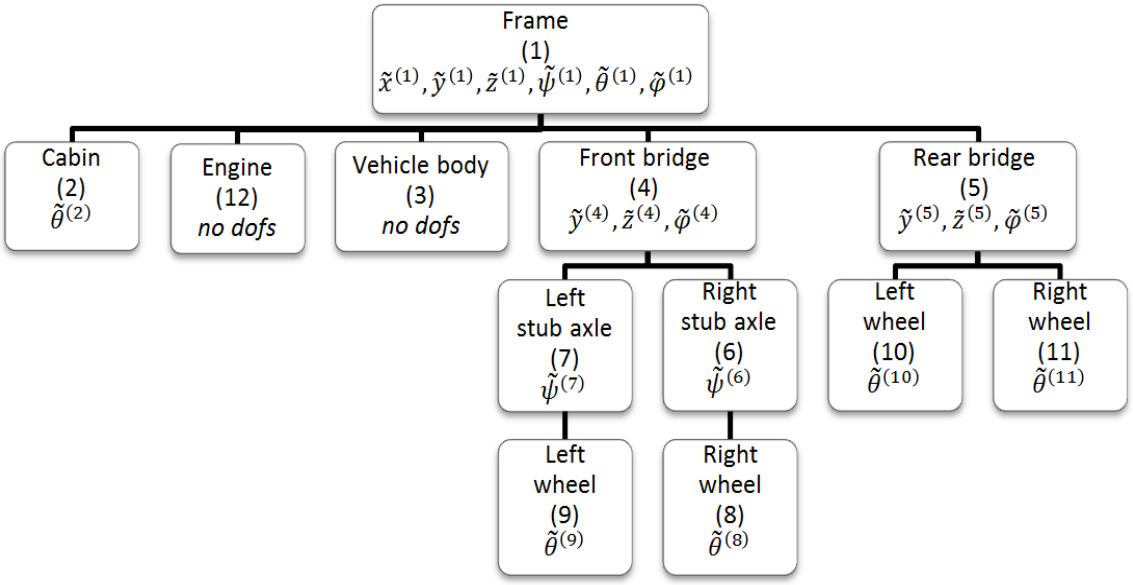

Figure 4 Models of the sub-assemblies forming the tree structure of the considered multibody system, where: (p) – body number in the multibody system; $\tilde{x}^{(p)}, \tilde{y}^{(p)}, z^{(p)}, \tilde{\psi}^{(p)}, \tilde{\theta}^{(p)}, \tilde{\varphi}^{(p)}$ – generalized coordinates of this body $(p = 1, \ldots, 12)$ described in relation to the preceding body

The frame model is a root of the tree, and its motion is described in respect to a global reference coordinate system $\{0\}$. the generalized coordinates of the frame model are displacements of the origin of the coordinate system $\{1\}$ – longitudinal $\tilde{x}^{(1)}$, lateral $\tilde{y}^{(1)}$, and vertical $\tilde{z}^{(1)}$ determined in the coordinate system $\{\square\}$ and the successive angles of rotation of this model around the axis (unit vectors) $\hat{Z}^{(1)}$, $\hat{Y}^{(1)}$, and $\hat{X}^{(1)}$ of the coordinate system $\{1\}$ – yaw $\tilde{\psi}^{(1)}$, pitch $\tilde{\theta}^{(1)}$,

and roll $\tilde{\varphi}^{(1)}$. The other models of sub-assemblies are connected directly or indirectly with the frame respectively.
In the doctoral dissertation [10], the detailed description of the process of mathematical modeling of the analyzed vehicle leading to formulation of the equations of motion is presented, and they can be written as:

$$\begin{cases} \boldsymbol{A}(t,\boldsymbol{q})\ddot{\boldsymbol{q}} - \boldsymbol{D}\boldsymbol{r} = \boldsymbol{f}(t,\boldsymbol{q},\dot{\boldsymbol{q}}) \\ \boldsymbol{D}^T\ddot{\boldsymbol{q}} = \boldsymbol{w} \end{cases} \tag{2}$$

where: t – time, $\boldsymbol{q}, \dot{\boldsymbol{q}}, \ddot{\boldsymbol{q}}$ – vectors of generalized coordinates, velocities and accelerations of considered mathematical model; $\boldsymbol{A}$ – mass matrix; $\boldsymbol{D}$ – matrix of coefficients corresponding to particular reaction forces; $\boldsymbol{r}$ – vector of unknown reaction forces; $\boldsymbol{f}$ – vector of generalized forces and derivatives of kinetic energy, potential energy, Rayleigh's dissipation function; $\boldsymbol{w}$ – vector of right sides of constraint equations.
To determine reaction forces and moments of interacting of the road surface on the vehicle wheel tires Pacejka's tire model was used [8]. Those reactions are applied at a contact point C of the tire model with the road surface. Detailed algorithms for modeling of the road surface, and algorithms which allow determining the position of contact point C in the coordinate system {□} are presented in next section.

4 MATHEMATICAL MODEL OF THE UNEVEN ROADS

For the purpose of the developed method, two ways of road surface modeling including occurrence of possible unevenness of any shape, were proposed.

4.1 The continuous model of the road surface

In the continuous model, the Bicubic interpolation [5] was used for the mathematical representation of the road surface, thus for determining the three dimensional interpolation surface. The input data are here the points in the three dimensional space – so called control points (interpolation nodes). The points located between these nodes are searched.
Let $P'_{i,j}$ and P' mean the xy plane projections of the control point $P_{i,j}(x_i, y_i, z_i)$ and the searched point $P(x_P, y_P, z_P)$ respectively, being on the interpolated surface, of which first two coordinates x_P and y_P are known. Then, the third coordinate z_P of the searched P point is determined by transforming the given grid cell specified by points $P'_{i,j}$, $P'_{i+1,j}$, $P'_{i+1,j+1}$ $P'_{i,j+1}$, into the square of the side length equal to 1 (Figure 5).

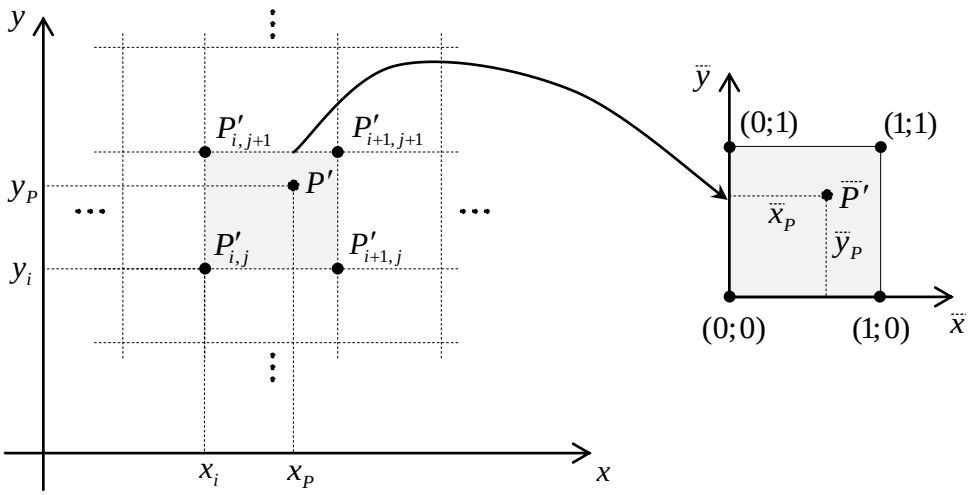

Figure 5 Transforming the selected grid cell

After transformations, coordinate z_P is calculated according to the formula:

$$z_P = f(x_P, y_P) = \bar{z}_P = \bar{f}(\bar{x}_P, \bar{y}_P) = \sum_{i=0}^{3}\sum_{j-0}^{3} a_{i,j}\bar{x}_P^i \bar{y}_P^i \,, \tag{3}$$

where: $\left.\begin{aligned} \bar{x}_P &= \frac{x_P - x_i}{x_{i+1} - x_i} \\ \bar{y}_P &= \frac{y_P - y_j}{y_{i+1} - y_j} \end{aligned}\right\} \in \langle 0;1 \rangle$ $\left.\begin{aligned} \bar{x}_P &= \frac{x_P - x_i}{x_{i+1} - x_i} \\ \bar{y}_P &= \frac{y_P - y_j}{y_{j+1} - y_j} \end{aligned}\right\} \in \langle 0;1 \rangle$ are the new coordinates of point P.

Formula (3) contains 16 unknown coefficients $a_{i,j}$, which are determined according to the method described in the doctoral dissertation [10].

From analyses made within the scope of the cited doctoral dissertation, it results that smooth interpolation surfaces are obtained when the continuous model is used, and they have an advantageous influence on efficiency of the calculation process performed in the scope of the analysis of the vehicle dynamics. However, the continuous model does not allow imitating unevenness of the road surface, which fragments are flat in some places (e.g. a vehicle drives through a speed bump on one side, and on the other it drives over the flat surface). In such a case, the discrete model should be taken into account.

4.2 The discrete model of the road surface

In the discrete model of the road surface developed by the author of the cited doctoral dissertation, it was assumed that this surface is modelled by the surface area built out of triangles (Figure 6).

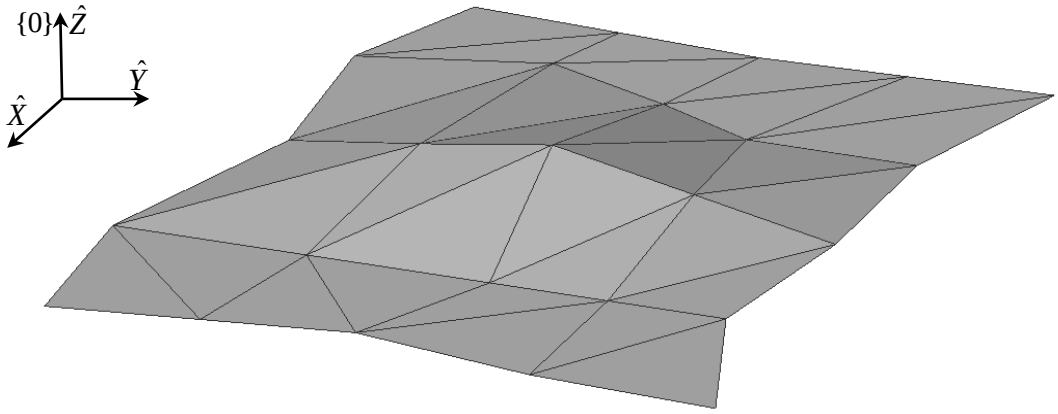

Figure 6 Example of the road surface fragment modelled by triangles

A number of triangles and their sizes are selected to represent the real shape of the road surface as accurately as possible.

The surface area made of the triangles can be defined on the basis of two sets:

1. $S^{(P)} = \{P_1(x_1, y_1, z_1), ..., P_i(x_i, y_i, z_i), ..., P_n(x_n, y_n, z_n)\}$ – a set of all points from which the triangles are built, where $P_i(x_i, y_i, z_i)$ $\mathrm{P_i(x_i, y_i, z_i)}$;
2. $S^{(v)} = \{\mathbf{v}^{(1)}, ..., \mathbf{v}^{(i)}, ..., \mathbf{v}^{(m)}\}$ – a set of 3-element vectors defining all the triangles, that is $\mathbf{v}^{(i)} = \left[v_1^{(i)} \quad v_2^{(i)} \quad v_3^{(i)}\right]^T$, where $v_1^{(i)}, v_2^{(i)}, v_3^{(i)} \in \{1, ..., n\}$ are indexes of the points (from the $\mathrm{S^{(P)}}$ set) being vertexes i-th of this triangle. It means mathematically that for each element of the $S^{(v)}$ set a mapping function, which indicates that the $\mathbf{v}^{(i)}$ element from the $S^{(v)}$ set describes a triangle of vertexes $P_{v_1^{(i)}}, P_{v_2^{(i)}}, P_{v_3^{(i)}}$, was determined in a form of: $\mathbf{v}^{(i)} \mapsto \{P_{v_1^{(i)}}, P_{v_2^{(i)}}, P_{v_3^{(i)}}\}$ $\mathrm{v^{(i)} \mapsto \{P_{v_1^{(i)}}, P_{v_2^{(i)}}, P_{v_3^{(i)}}\}}$.

It should be emphasised that one element (a point) from the $\mathrm{S^{(P)}}$ set can be a common element (a point) for two or more triangles simultaneously.

As in the continuous model, a position of the $P(x_P, y_P, z_P)$ point being in the surface area in question is searched and its coordinates x_P and y_P are known (Figure 7). The z_P coordinate of point P can be determined in a way described further in this article.

Let point P be in the area of the k triangle of vertexes $\mathrm{P_{v_1^{(k)}}, P_{v_2^{(k)}}, P_{v_3^{(k)}}}$ (Figure 7).

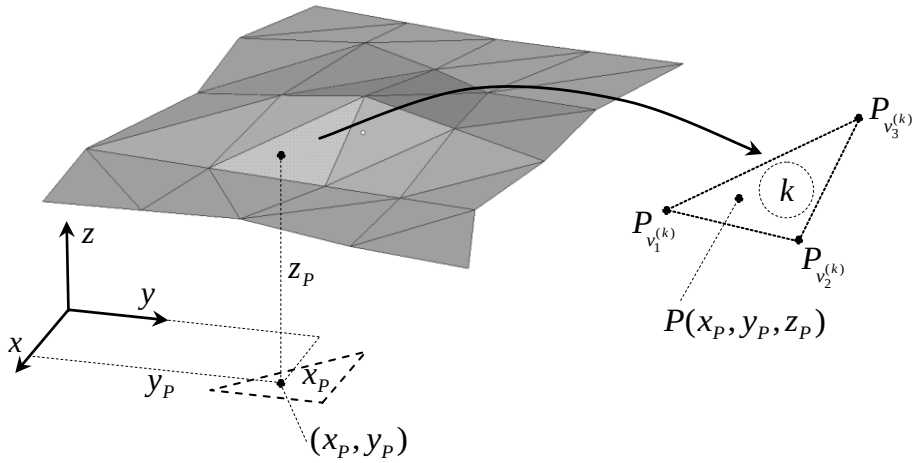

Figure 7 Position of the searched point P on the surface area modelled by the triangles P

The vertexes of this triangle determine the plane of which the normal equation has the following form:

$$e_x^{(k)}x + e_x^{(k)}y + e_x^{(k)}z + \delta^{(k)} = 0, \tag{4}$$

where:

$e_x^{(k)}$, $e_y^{(k)}$, $e_z^{(k)}$ – elements of the $\hat{\mathbf{e}}^{(k)}$ versor normal to the k triangle surface area,

$\delta^{(k)} = -\left(e_x^{(k)}x_l + e_y^{(k)}y_l + e_z^{(k)}z_l\right)$, where l should be taken as any number from set $\left\{v_1^{(k)}, v_2^{(k)}, v_3^{(k)}\right\}$.

Versor $\hat{\mathbf{e}}^{(k)}$ can be determined by the vector product:

$$\hat{\mathbf{e}}^{(k)} = \frac{\mathbf{p}_{1,2}^{(k)} \times \mathbf{p}_{1,3}^{(k)}}{\left|\mathbf{p}_{1,2}^{(k)} \times \mathbf{p}_{1,3}^{(k)}\right|}, \tag{5}$$

where:

$\mathrm{p}_{1,2}^{(\mathrm{k})}$ – the vector with the beginning in point $P_{v_1^{(k)}}$ and the end in point $P_{v_2^{(k)}}$,

$\mathbf{p}_{1,3}^{(k)}$ – the vector with the beginning in point $\mathrm{P}_{\mathrm{v}_1^{(\mathrm{k})}}$ and the end in point $P_{v_3^{(k)}}$.

Having the plane equation determined in (4), the searched $\mathrm{z_P}$ coordinate of the point P can be determined from the formula:

$$z_P = -\frac{e_x^{(k)}x_P + e_y^{(k)}y_P + \delta^{(k)}}{e_z^{(k)}}, \tag{6}$$

for $e_z^{(k)} \neq 0$, excluding the situation when the *k* triangle plane is perpendicular to the *xy* plane – those cases do not concern this work.

In the described procedure, it was assumed that the vertexes of the triangle, on which there is point *P*, are known. However, identification of this triangle is not a trivial task. It becomes especially difficult in a case of computer simulations where short time of calculations is usually significant. Therefore, it is essential to develop an appropriate algorithm of the triangle identification of the surface area in question. The trivial solution of the triangle identification problem consists of searching the whole set of triangles $S^{(v)}$ and checking if the searched element is in the surface area of this triangle. In this case, for each triangle ($k = 1,...,m$) the plane equation (4) should be determined, and it should be checked if the *P* point is in its fragment specified by vertexes $\mathrm{P}_{\mathrm{v}_1^{(\mathrm{k})}}, \mathrm{P}_{\mathrm{v}_2^{(\mathrm{k})}}, \mathrm{P}_{\mathrm{v}_3^{(\mathrm{k})}}$. Such an algorithm does not belong to efficient regarding calculating, and because of three dimensionality it may prove to be problematic. Much better results can be obtained by reducing the problem to a two dimensional issue and narrowing appropriately the set of the searched triangles. In this work, the developed algorithm was divided into two stages: "reducing the problem to a two dimensional issue" and "limiting the search set". These stages are detailed explained in doctoral dissertation [10].

4.3 Normal versor to modeled road surface

Each of the presented road surface models can be characterized by an equation of the assumed mapping surface in the form of:

$$z = z(x, y). \tag{7}$$

In further considerations it is assumed that in any point *P* of this surface of coordinates x_P, y_P, z_P determined in any immovable coordinate system {0} assumed, being a reference system (Figure 8), normal versor $\hat{\mathbf{e}}$ to this surface is known.

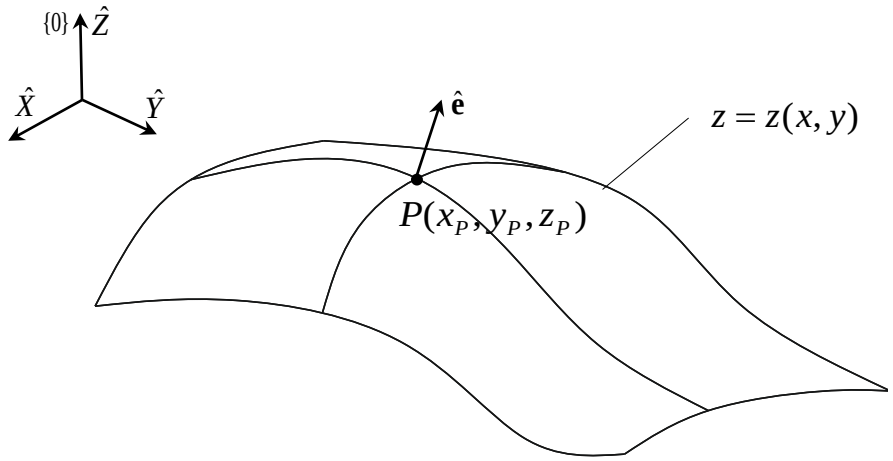

Figure 8. Normal versor $\hat{\mathbf{e}}$ to the mapping surface in point $P(x_P, y_P, z_P)$

According to the suggestions presented in work [3], in the case of the continuous model of the road surface, in the neighborhood of point *P* (Figure 9), it is assumed that there are four auxiliary points of the coordinates determined in reference system {0} as:

$$\begin{aligned} &P^{(x+)}\big(x_P + \Delta, y_P, z(x_P + \Delta, y_P)\big), \\ &P^{(x+)}\big(x_P - \Delta, y_P, z(x_P - \Delta, y_P)\big), \\ &P^{(y+)}\big(x_P, y_P + \Delta, z(x_P, y_P + \Delta)\big), \\ &P^{(y-)}\big(x_P, y_P - \Delta, z(x_P, y_P - \Delta)\big). \end{aligned} \tag{8}$$

Then, the normal versor can be determined according following formula:

$$\hat{\mathbf{e}} = \frac{\mathbf{r}^{(x)} \times \mathbf{r}^{(y)}}{\left| \mathbf{r}^{(x)} \times \mathbf{r}^{(y)} \right|}, \tag{9}$$

where: $\mathbf{r}^{(x)}$ – vector with the origin in point $P^{(x-)}$ and the end in point $P^{(x+)}$,
$\mathbf{r}^{(y)}$ – vector with the origin in point $P^{(y-)}$ and the end in point $P^{(y+)}$,
Δ [m] – short distance (in the work it was assumed $\Delta = 0{,}01$ m).

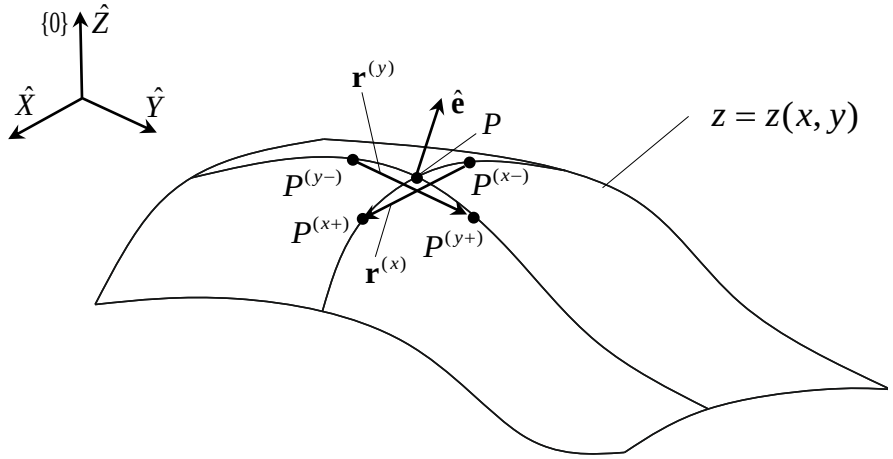

Figure 9. The continuous model of the road surface – determining normal versor $\hat{\mathbf{e}}$ to the mapping surface in point $P(x_P, y_P, z_P)$

In the case of the discrete model of the road surface, based on the triangles or rectangles implemented, the normal versor $\hat{\mathbf{e}}$ can be determined on basis of the known basic geometrical relationships.

5 ALGORITHMS OF ITERATIVE DETERMINING THE CONTACT POINT POSITION

While analyzing vehicle dynamics forces and reaction torques, acting on models of their tires from the road surface, must be considered appropriately. In real conditions the tire contact with this frequently uneven surface takes place within the definite area. When the tire is modeled, the contact surface is usually limited to a point [3], [4], [9]. The authors of this work followed also this procedure, assuming that the modeled tire – considered in a form of a deformable rim – will contact with the mapping surface of the road surface in a definite point

As it is known in any point of the mapping surface a plane tangent to it can be placed. In this method, as it was done by the authors of articles [3], [4], [9], [11], it has been assumed that the tire will be modeled in a form of a deformable rim, obtained as a result of a longitudinal cut of this tire in its symmetry plane. This rim in the deformable part adheres to the mapping surface – even so for needs of the model it is assumed that its contact with this surface takes place in the definite point (it is the C contact point). In a non-deformable form this rim is a circle of the O symmetry center, overlapping with the symmetry center of the non-deformed tire. In the contact point C there is also plane Π – tangent to the mapping surface (Figure 10). On basis of the suggestions included in work [11], in addition to the reference system $\{0\}$ mentioned already, two local coordinate systems – $\{w\}$ and $\{r\}$ were assumed. The movable system $\{w\}$ is connected with the rim. Its origin was placed in the O symmetry center of the non-deformed rim, versor $\hat{Y}_w$ overlaps with its axis of rotation (and therefore, also with the axis of rotation of the modeled tire), and versor $\hat{X}_w$ remains parallel to plane Π during the whole time of vehicle motion. The origin of immovable system $\{r\}$ overlaps with the contact point C, its versor $\hat{Z}_r$ is normal to plane Π – and also to the mapping surface (angle γ between it and versor $\hat{Z}_w$ is an inclination angle of the tire), whereas versor $\hat{X}_r$ lying in this plane remains pararlel to versor $\hat{X}_w$ of the $\{w\}$ system during the vehicle motion. While modeling an interaction of the road surface on the tire, it is assumed that in the contact point C the following forces and reaction torques are applied: $\mathbf{F}_x$ – the reaction force longitudinal, $\mathbf{F}_y$ – the reaction force lateral, $\mathbf{F}_z$ – the reaction force normal to the mapping surface (plane Π), $\mathbf{M}_x$ – the overturning torque, $\mathbf{M}_y$ – the rolling resistance torque, $\mathbf{M}_z$ – the aligning torque. Their directions are consistent with the directions of versors of the $\{r\}$ system. Values of these forces and torques are calculated by use of formulas offered by so called the Pacejka tire model [6], [7], [8] taken into account in the method proposed.

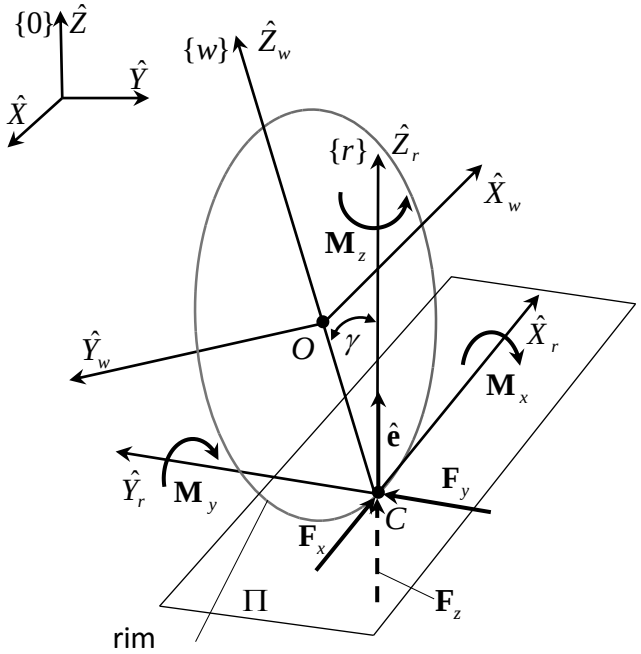

Figure 10. Location of local systems $\{w\}$ i $\{r\}$

While performing an analysis of the vehicle dynamics, it is assumed that a position of the $\{w\}$ system origin is known at any time of its motion (as known, identical with the O symmetry center of the non-deformed rim) and orientation of its versor $\hat{Y}_w$ in the $\{0\}$ reference system. The authors of the article also made the same assumption [4]. Additionally, the position of the contact point C, being the beginning of the $\{r\}$ system in this system and orientation of versors of this system in the $\{0\}$ reference system must be known. Iterative determination of this position and orientation is a subject of the algorithms presented in this work. When a distance of origins of systems $\{w\}$ and $\{r\}$ is known, values of forces and reaction torques acting on the tire from the road surface can be determined by use of the Pacejka tire model. Knowledge about orientation of versors of the $\{r\}$ system in the $\{0\}$ reference system will allow to find directions of acting of these forces and torques – this information is needed to make an analysis of the dynamics of the vehicle in question while using the Pacejka tire model mentioned or other tire models, relying on the similar assumptions regarding a way of applying forces and torques.

Two algorithms, intended for determining the position of the contact point C and orientation of the vectors of the $\{r\}$ coordinate system were proposed. In accordance with intention of the authors the names of the algorithms are to refer to the essence of a procedure assumed in each case. The Plane algorithm is designed for the continuous model of the road surface, whereas the 4Points algorithm –for the discrete model of this surface.

6 ALGORITHM PLANE

Determining the position of the contact point C by the Plane algorithm refers to performing a definite number of iterations. Execution of the first of them is presented in Figure 11.

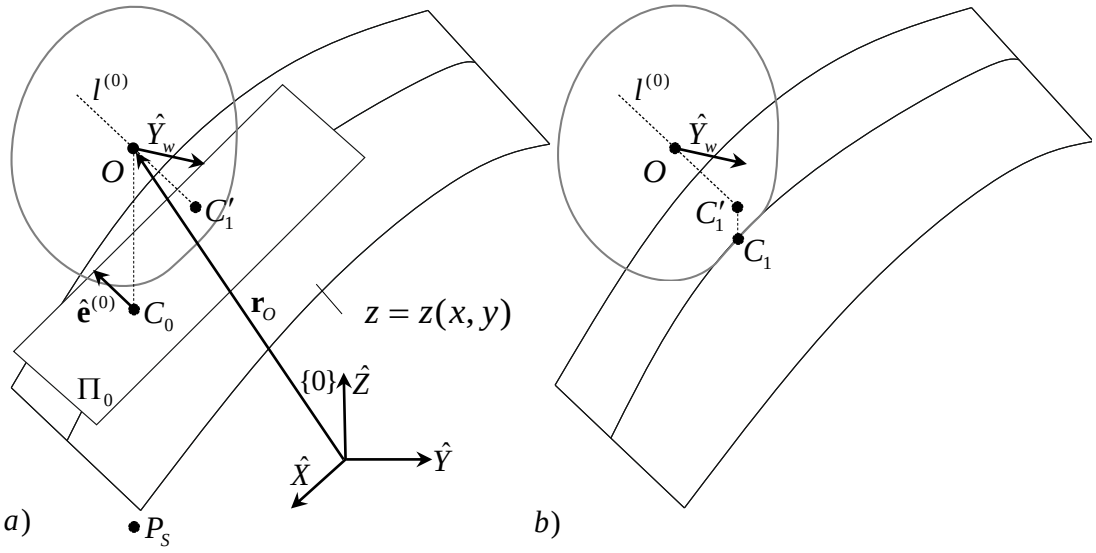

Figure 11. The Plane algorithm – the first approximation of the position of the contact point C

In the neighborhood of the O symmetry center of the non-deformed rim (Figure 11(a)) a start point P_S of coordinates x_S, y_S, z_S, defined in the {0} reference system is selected. In this work it has been assumed that it is the O point. Then, coordinates of the C_0 point, being an orthogonal projection to the mapping surface, are determined in this system:

$$C_0 = \left(x_{C_0}, y_{C_0}, z_{C_0}\right) = \left(x_O, y_O, z(x_O, y_O)\right). \tag{10}$$

A next step is to determine plane Π_0 tangent to the mapping surface in the C_0 point. A point-normal equation of this plane can be presented in the following form (similar to eq. 4):

$$e_x^{(0)} x + \quad e_y^{(0)} y + \quad e_z^{(0)} z + \delta^{(0)} = 0, \tag{11}$$

where: $e_x^{(0)}$, $e_y^{(0)}$, $e_z^{(0)}$ are components of the $\hat{\mathbf{e}}^{(0)}$ versor normal to the mapping surface in the C_0 point determined in the {0} reference system,

$$\delta^{(0)} = -\left(\quad e_x^{(0)} x_{C_0} + \quad e_y^{(0)} y_{C_0} + \quad e_z^{(0)} z_{C_0} \right).$$

Point $C_1'\left(x_{C_1'}, y_{C_1'}, z_{C_1'}\right)$, in which straight line $l^{(0)}$ going through the O points pierces plane Π_0 perpendicularly, is determined next . Its coordinates in the {0} reference system can be determined by the position vector (Figure 11(b)) as:

$$\mathbf{r}_{C_1'} = \quad \mathbf{r}_O - d_0 \quad \hat{\mathbf{e}}^{(0)} \quad , \tag{12}$$

where: $d_0 = \left| e_x^{(0)} x_O + e_y^{(0)} y_O + e_z^{(0)} z_O + \delta^{(0)} \right|$ – a distance of points O and C_1'.

As a result, these coordinates can be presented as:

$$C_1'\left(x_{C_1'}, y_{C_1'}, z_{C_1'}\right) = C_1'\left(x_O - e_x^{(0)} d_0, y_O - e_y^{(0)} d_0, z_O - e_z^{(0)} d_0\right). \tag{13}$$

Then, the coordinates of point C_1, being the first approximation of the contact point C, are determined:

$$C_1\left(x_{C_1}, y_{C_1}, z_{C_1}\right) = C_1\left(x_{C_1'}, y_{C_1'}, z\left(x_{C_1'}, y_{C_1'}\right)\right). \tag{14}$$

To determine n-th approximation of the position of the contact point C the algorithm can be generalized to $i = 1, \ldots, n$ iterations writing formulas (13) and (14) as:

$$C_i'\left(x_{C_i'}, y_{C_i'}, z_{C_i'}\right) = C_1'\left(x_O - e_x^{(i-1)} d_{i-1}, y_O - e_y^{(i-1)} d_{i-1}, z_O - e_z^{(i-1)} d_{i-1}\right) \quad (15)$$

and:

$$C_i\left(x_{C_i}, y_{C_i}, z_{C_i}\right) = C_i\left(x_{C_i'}, y_{C_i'}, z\left(x_{C_i'}, y_{C_i'}\right)\right). \quad (16)$$

The n value is determined by the criterion:

$$\sqrt{\left(x_{C_{n-1}} - x_{C_n'}\right)^2 + \left(y_{C_{n-1}} - y_{C_n'}\right)^2 + \left(z_{C_{n-1}} - z_{C_n'}\right)^2} \leq \varepsilon, \quad (17)$$

where: ε – an assumed acceptable absolute error of calculations.
The versor $\hat{X}_r^{(n)}$ of the $\{r\}$ system in the reference system $\{0\}$ can be determined by the formula (Figure 10):

$$\hat{X}_r^{(n)} = \frac{\hat{Y}_w \times \hat{\mathbf{e}}^{(n)}}{|\hat{Y}_w \times \hat{\mathbf{e}}^{(n)}|}, \quad (18)$$

and then other versors as:

$$\begin{aligned} \hat{Y}_r^{(n)} &= \hat{X}_r \times \hat{\mathbf{e}}^{(n)}, \\ \mathrm{Z}_r^{(n)} &= \hat{\mathbf{e}}^{(n)}. \end{aligned} \quad (19)$$

7 ALGORITHM 4POINTS

As it has been found out the Plane algorithm is used in the case of the continuous model of the road surface. However, in the case of the discrete model when some fragments of the surface are flat, determining the position of the contact point C by its use may not be accurate enough. Such a situation is presented in Figure 12.

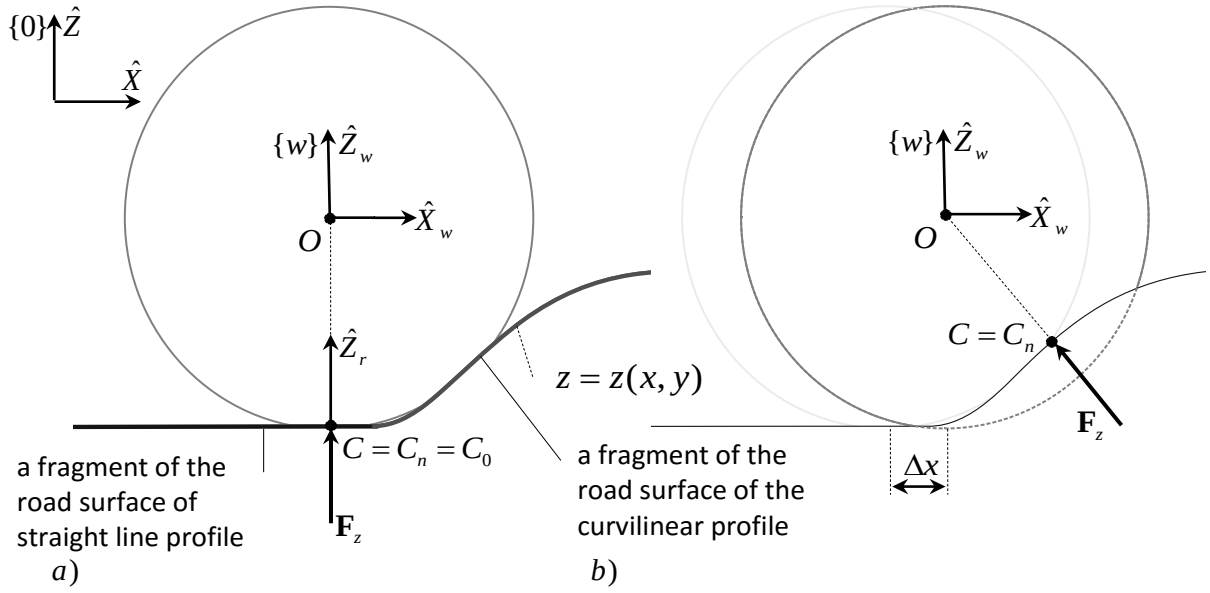

Figure 12. The Plane algorithm – the determined positions of the contact point C: a) at beginning of running the modeled tire over unevenness, b) after covering distance Δx

While considering the position of the modeled tire presented in Figure 12(a), it can be noticed that the contact point C is the orthogonal projection of the symmetry center O of the non-deformed rim on the flat fragment of the road surface. It can be stated that condition (17),

determining completion of calculations, is met after the first iteration, because already then it is $\sqrt{\left(x_{C_{n-1}-}x_{C_n'}\right)^2+\left(y_{C_{n-1}-}y_{C_n'}\right)^2+\left(z_{C_{n-1}-}z_{C_n'}\right)^2}=0<\varepsilon$. Here, an undesirable effect is too late reaction of the rim to changeable surface profile. Since the Plane algorithm does not allow to take the rim contact with the road fragment of the curvilinear profile (marked in the figure) into account early enough, so a direction of the normal reaction force $\mathbf{F}_z$ (acting on the rim in accordance with the $\hat{Z}_r$ versor direction) turns out to be incorrect. It can be stated that this direction "does not keep up with a new situation on the road". The normal reaction force changes its direction after the modeled tire has covered the Δx distance (Figure 12(b)) – so too late – and this change is rather rapid. Therefore, it has been required to develop an algorithm, which would enable to determine an appropriate position of the contact point C, ensuring that shape changes of the mapping surface are considered early enough, what would provide more accurate direction of the $\mathbf{F}_z$ normal reaction force, because closer to real one.

At the beginning of realization of the new algorithm named 4Points in planes $\hat{X}_w,\hat{Z}_w$ and $\hat{Y}_w,\hat{Z}_w$ of the $\{w\}$ system there are four auxiliary points $O^{(x+)},O^{(x-)},O^{(y+)},O^{(y-)}$ assumed, respectively (Figure 13).

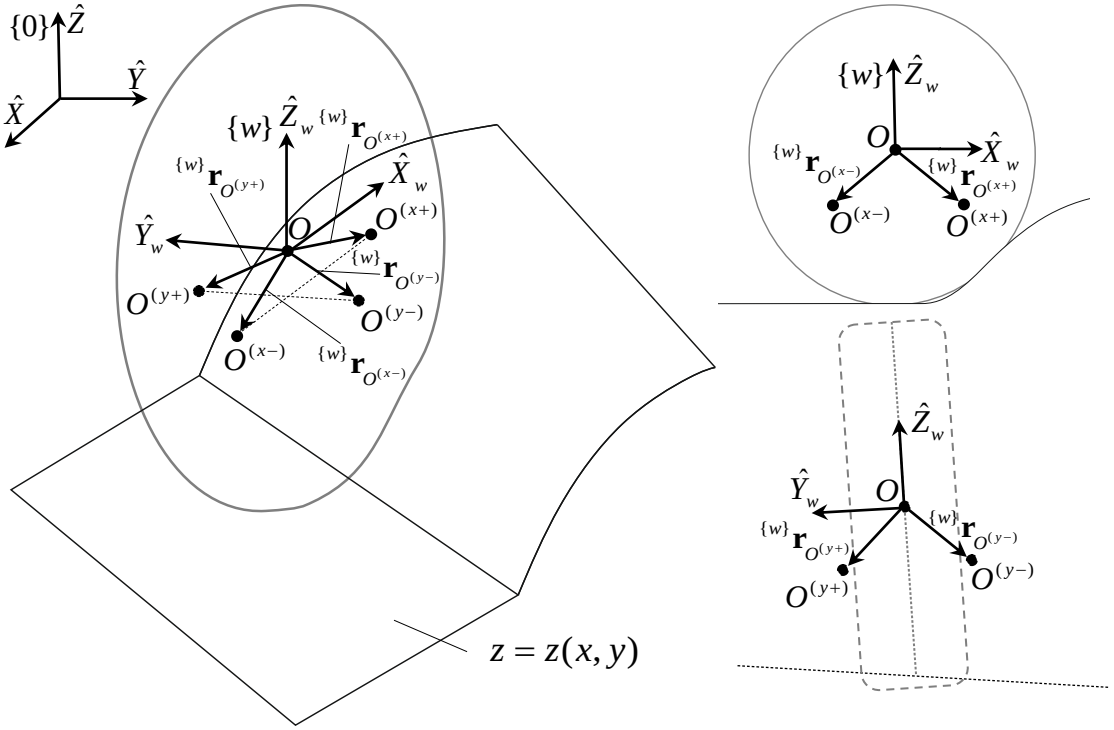

Figure 13. Algorithm 4Points – positions of the auxiliary points

Coordinates of them in the $\{w\}$ system can be determined by the position vectors of the homogenous coordinates:

$$
{}^{\{w\}}\mathbf{r}^{*}_{O^{(x+)}}=\begin{bmatrix}{}^{\{w\}}\mathbf{r}_{O^{(x+)}}\\1\end{bmatrix},\qquad {}^{\{w\}}\mathbf{r}_{O^{(x+)}}=\begin{bmatrix}\Delta x\\0\\-\Delta z\end{bmatrix},
$$
$$
{}^{\{w\}}\mathbf{r}^{*}_{O^{(x-)}}=\begin{bmatrix}{}^{\{w\}}\mathbf{r}_{O^{(x-)}}\\1\end{bmatrix},\qquad {}^{\{w\}}\mathbf{r}_{O^{(x-)}}=\begin{bmatrix}-\Delta x\\0\\-\Delta z\end{bmatrix},
\tag{20}
$$

$$
{}^{\{w\}}\mathbf{r}^{*}_{O^{(y+)}} = \begin{bmatrix} {}^{\{w\}}\mathbf{r}_{O^{(y+)}} \\ 1 \end{bmatrix}, \qquad {}^{\{w\}}\mathbf{r}_{O^{(y+)}} = \begin{bmatrix} 0 \\ \Delta y \\ -\Delta z \end{bmatrix},
$$

$$
{}^{\{w\}}\mathbf{r}^{*}_{O^{(y-)}} = \begin{bmatrix} {}^{\{w\}}\mathbf{r}_{O^{(y-)}} \\ 1 \end{bmatrix}, \qquad {}^{\{w\}}\mathbf{r}_{O^{(y-)}} = \begin{bmatrix} 0 \\ -\Delta y \\ -\Delta z \end{bmatrix},
$$

where: $\Delta x, \Delta y, \Delta \mathrm{z}$ [m] – distances resulting from tire size (in the work the following values were assumed: $\Delta x = 0{,}17, \Delta y = 0{,}07, \Delta \mathrm{z} = 0{,}1$).

Then, the vectors of the homogenous coordinates determining the position of the auxiliary points in the {0} reference system, can be determined as:

$$
\begin{aligned}
\mathbf{r}^{*}_{O^{(x+)}} &= \mathbf{T}_w \, {}^{\{w\}}\mathbf{r}^{*}_{O^{(x+)}}, \mathbf{r}^{*}_{O^{(x+)}} = \begin{bmatrix} \mathbf{r}_{O^{(x+)}} \\ 1 \end{bmatrix}, \qquad \mathbf{r}_{O^{(x+)}} = \begin{bmatrix} x_{O^{(x+)}} \\ y_{O^{(x+)}} \\ z_{O^{(x+)}} \end{bmatrix}, \\
\mathbf{r}^{*}_{O^{(x-)}} &= \mathbf{T}_w \, {}^{\{w\}}\mathbf{r}^{*}_{O^{(x-)}}, \mathbf{r}^{*}_{O^{(x-)}} = \begin{bmatrix} \mathbf{r}_{O^{(x+)}} \\ 1 \end{bmatrix}, \qquad \mathbf{r}_{O^{(x-)}} = \begin{bmatrix} x_{O^{(x-)}} \\ y_{O^{(x-)}} \\ z_{O^{(x-)}} \end{bmatrix}, \\
\mathbf{r}^{*}_{O^{(y+)}} &= \mathbf{T}_w \, {}^{\{w\}}\mathbf{r}^{*}_{O^{(y+)}}, \mathbf{r}^{*}_{O^{(y+)}} = \begin{bmatrix} \mathbf{r}_{O^{(y+)}} \\ 1 \end{bmatrix}, \qquad \mathbf{r}_{O^{(x+)}} = \begin{bmatrix} x_{O^{(y+)}} \\ y_{O^{(y+)}} \\ z_{O^{(y+)}} \end{bmatrix}, \\
\mathbf{r}^{*}_{O^{(y-)}} &= \mathbf{T}_w \, {}^{\{w\}}\mathbf{r}^{*}_{O^{(y-)}}, \mathbf{r}^{*}_{O^{(y-)}} = \begin{bmatrix} \mathbf{r}_{O^{(y-)}} \\ 1 \end{bmatrix}, \qquad \mathbf{r}_{O^{(y-)}} = \begin{bmatrix} x_{O^{(y-)}} \\ y_{O^{(y-)}} \\ z_{O^{(y-)}} \end{bmatrix},
\end{aligned}
\tag{21}
$$

where: $\mathbf{T}_w$ – a known transformation matrix from system $\{w\}$ to reference system {0}.

In further procedure auxiliary points $O^{(x+)}, O^{(x-)}, O^{(y+)}, O^{(y-)}$ are projected on the mapping surface (Figure 14(a)), and next the homogenous vectors, determining coordinates of their projections $O'^{(x+)}, O'^{(x-)}, O'^{(y+)}, O'^{(y-)}$ in the {0} reference system are determined as:

$$
\begin{aligned}
\mathbf{r}^{*}_{O'^{(x+)}} &== \begin{bmatrix} \mathbf{r}_{O'^{(x+)}} \\ 1 \end{bmatrix}, \qquad \mathbf{r}_{O^{(x+)}} = \begin{bmatrix} x_{O'^{(x+)}} \\ y_{O'^{(x+)}} \\ z_{O'^{(x+)}} \end{bmatrix} = \begin{bmatrix} x_{O^{(x+)}} \\ y_{O^{(x+)}} \\ z\left(x_{O^{(x+)}}, y_{O^{(x+)}}\right) \end{bmatrix}, \\
\mathbf{r}^{*}_{O'^{(x-)}} &== \begin{bmatrix} \mathbf{r}_{O'^{(x-)}} \\ 1 \end{bmatrix}, \qquad \mathbf{r}_{O^{(x-)}} = \begin{bmatrix} x_{O'^{(x-)}} \\ y_{O'^{(x-)}} \\ z_{O'^{(x-)}} \end{bmatrix} = \begin{bmatrix} x_{O^{(x-)}} \\ y_{O^{(x-)}} \\ z(x_{O^{(x-)}}, y_{O^{(x-)}}) \end{bmatrix}, \\
\mathbf{r}^{*}_{O'^{(y+)}} &== \begin{bmatrix} \mathbf{r}_{O'^{(y+)}} \\ 1 \end{bmatrix}, \qquad \mathbf{r}_{O^{(y+)}} = \begin{bmatrix} x_{O'^{(y+)}} \\ y_{O'^{(y+)}} \\ z_{O'^{(y+)}} \end{bmatrix} = \begin{bmatrix} x_{O^{(y+)}} \\ y_{O^{(y+)}} \\ z(x_{O^{(y+)}}, y_{O^{(y+)}}) \end{bmatrix}, \\
\mathbf{r}^{*}_{O'^{(y-)}} &== \begin{bmatrix} \mathbf{r}_{O'^{(y-)}} \\ 1 \end{bmatrix}, \qquad \mathbf{r}_{O^{(y-)}} = \begin{bmatrix} x_{O'^{(y-)}} \\ y_{O'^{(y-)}} \\ z_{O'^{(y-)}} \end{bmatrix} = \begin{bmatrix} x_{O^{(y-)}} \\ y_{O^{(y-)}} \\ z(x_{O^{(y-)}}, y_{O^{(y-)}}) \end{bmatrix},
\end{aligned}
\tag{22}
$$

On basis of formula (9) the versor normal to plane Π, including the projections of the auxiliary points can be determined as:

$$
\hat{\mathbf{e}} = \frac{\mathbf{r}^{(x)}_{O'} \times \mathbf{r}^{(y)}_{O'}}{\left| \mathbf{r}^{(x)}_{O'} \times \mathbf{r}^{(y)}_{O'} \right|}, \tag{23}
$$

where: $\mathbf{r}^{(x)}_{O'} = \mathbf{r}_{O'^{(x+)}} - \mathbf{r}_{O'^{(x-)}}$ – vector of origin in point $O'^{(x+)}$ and end in point $O'^{(x-)}$,

$\mathbf{r}^{(y)}_{O'} = \mathbf{r}_{O'^{(y+)}} - \mathbf{r}_{O'^{(y-)}}$ – vector of origin in point $O'^{(y+)}$ and end in point $O'^{(y-)}$.

On basis of the determined normal versor **ê** and one of any selected auxiliary points $O'^{(x+)}, O'^{(x-)}, O'^{(y+)}, O'^{(y-)}$ the Π plane mentioned is sought for, of which the point-normal equation has a from:

$$e_x x + e_y y + e_z z + \delta = 0, \tag{24}$$

where: e_x, e_y, e_z are the components of the versor **ê** normal to plane Π determined in the {0} reference system,

$\delta = -\left(e_x x_{O'^{(x+)}} + e_y y_{O'^{(x+)}} + e_z z_{O'^{(x+)}}\right)$ if the selected point is $O'^{(x+)}$.

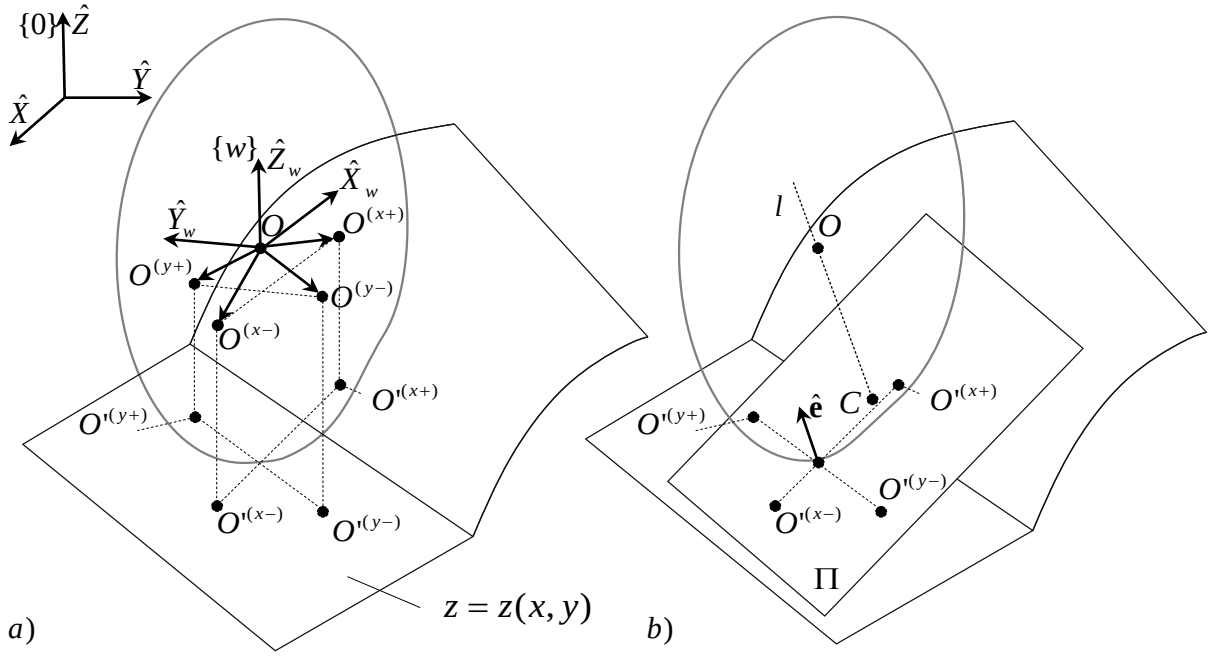

Figure 14. Algorithm 4Points – determining the orthogonal projections of the auxiliary points on the mapping surface

The sought contact point C is determined as a point in which straight line l going through the point O pierces the plane Π perpendicularly (Figure 14(b)). Its coordinates in the {0} reference system are determined as the components of the position vector:

$$\mathbf{r}_C = \mathbf{r}_O - d_0 \hat{\mathbf{e}}, \tag{25}$$

where: $d_0 = \left| e_x\, x_O + e_y\, y_O + e_z\, z_O + \delta \right|$ – a distance of points O and C.
As a result the coordinates of the contact point C can be determined as:

$$C(x_C, y_C, z_C) = C\left(x_O - e_x\, d_0, y_O - e_y\, d_0, z_O - e_z\, d_0\right). \tag{26}$$

Using this algorithm for the case illustrated in Figure 12(a), the position of the contact point C can be determined as presented in Figure 15. The corrected direction of reaction force $\mathbf{F}_z$ is presented in this figure.

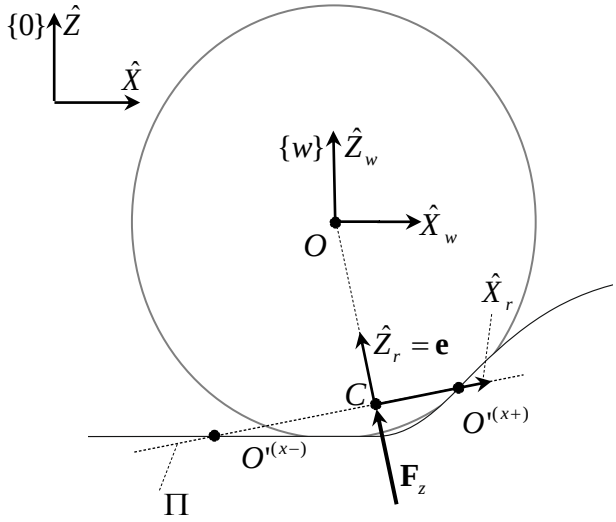

Figure 15. Algorithm 4Points – determining the position of the contact point C and the corrected direction of normal reaction force $\mathbf{F}_z$

The versor directions of the $\{r\}$ system are determined in a similar way as in the case of the Plane algorithm, that is according to relationships (18) and (19).

8 COMPUTER SIMULATIONS

A technical rescue vehicle, which can drive in the terrain conditions, was used for the analysis. Its physical model in a form of multibody system of open structure, built by use of joint coordinates defining a relative position of the modeled components, and a mathematical model corresponding to it, developed on basis of Lagrange equations formalism by use of homogenous transformation matrices [2], is presented in the doctoral dissertation [10]. Program Blender [12] was used to model the uneven road surface and to develop a model of the vehicle used in the computer animations.

In each case considered the modeled vehicle moved in the direction consistent with versor $\hat{X}$ of the {0} reference system. The vehicle initial speed was 5 km/h, and simulation duration time was 6s.

Example I

The assumed continuous model of the road surface in a form of a grid of control points is presented in figure 16. The boundary values of the coordinates of those points in the {0} reference system were following: $x_{min} = -2$; $x_{max} = 49$; $y_{min} = -8$; $y_{max} = 8$; $z_{min} = -0{,}8$; $z_{max} = 1{,}2$.

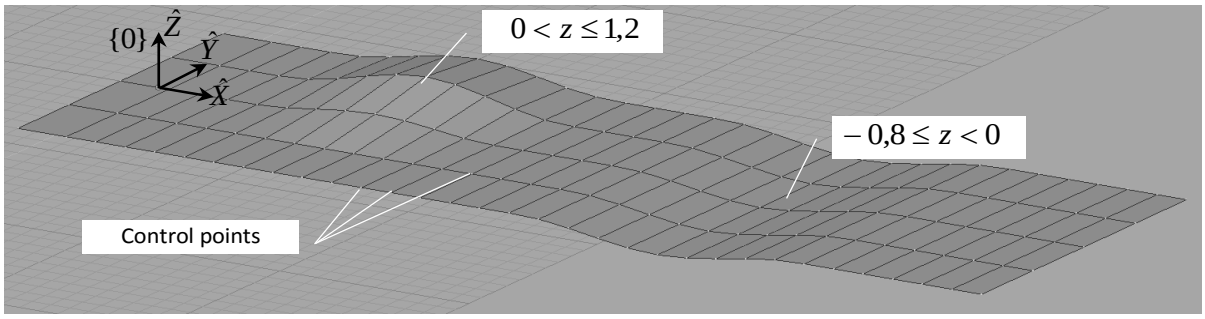

Figure 16. The control point grid in the case of the continuous model of the road surface

Within the computer animation performed vehicle drives over the uneven road surface of the shape as shown in Figure 17 were simulated.

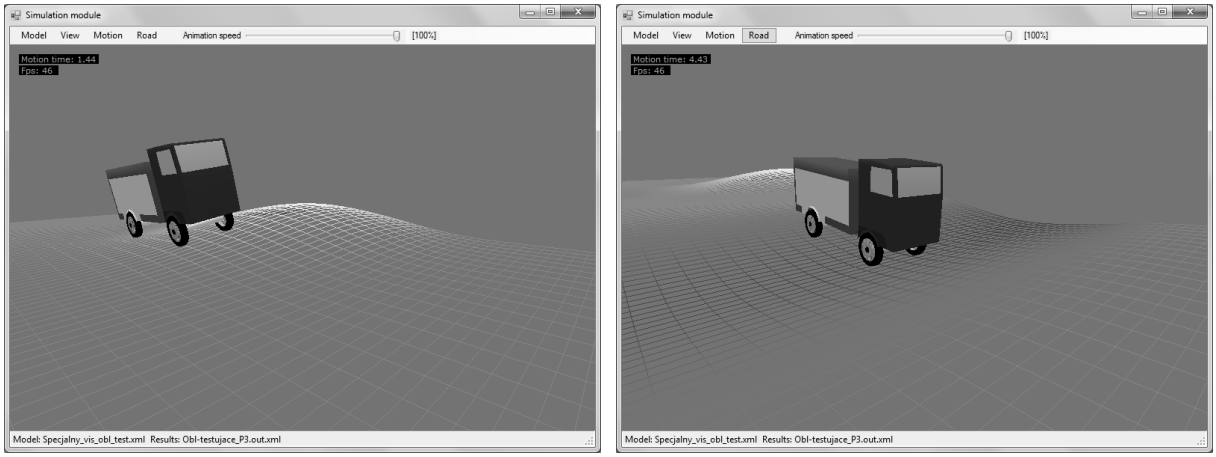

a) *b*)

Figure 17. Some screen shots made during the computer animation:
a) a phase of the vehicle going up to unevenness, b) a phase of going down from unevenness

Some examples of the calculation results which concern determining a vertical course of the gravity center displacement of the vehicle model (towards versor $\hat{Z}$ of the {0} reference system) – taking the Plane algorithm into account – are presented in Figure 18.

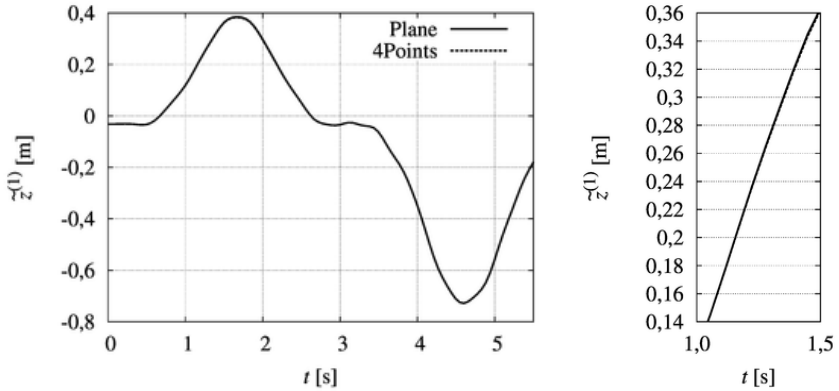

Figure 18. A course of the vertical displacement of the vehicle gravity center in the case of considering the continuous model of the road surface

This diagram was compared with the vertical course of this center, determined by using the 4Points algorithm. The results obtained are almost identical. Therefore, it may be concluded that in the case of smooth unevenness a selection of the algorithm has a slight influence on the computer simulation results obtained.

Example II

The assumed discrete model of the road surface in the form of the grid of the control points is presented in Figure 19. It consists of two flat fragments adjacent to a bump. Since there are no inclination of the surface in the direction consistent with versor $\hat{Y}$ of the {0} reference system, its model was made by use of rectangles placed as shown in the figure. The assumed boundary values of the grid points coordinates were following: $x_{min} = -2$; $x_{max} = 11{,}5$; $y_{min} = -2$; $y_{max} = 2$; $z_{min} = 0$; $z_{max} = 0{,}2$.

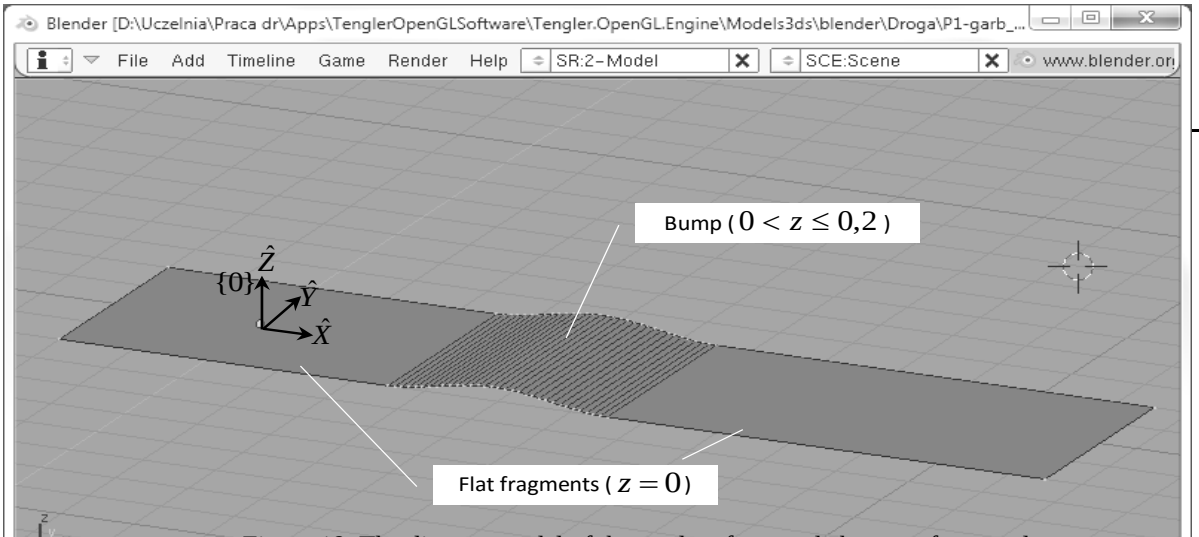

Figure 19. The discrete model of the road surface made by use of rectangles

Within the computer animation performed a drive of the vehicle over the bump was simulated (Figure 20).

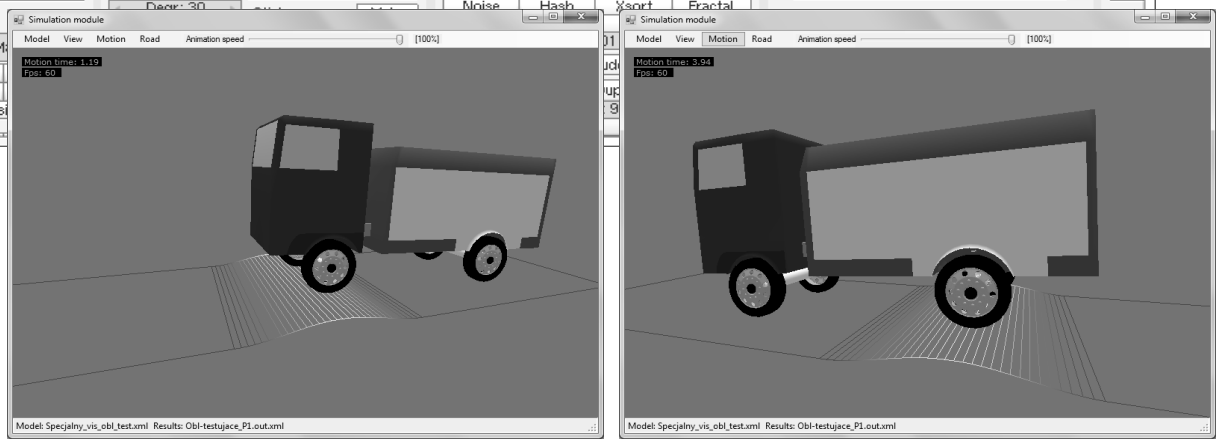

a) *b*)

Figure 20. Some screen shots made during the computer animation:
a) a phase of the vehicle going up the bump, b) a phase of the vehicle going down from the bump

Some examples of the calculations results which concern determining the vertical displacement course of the gravity center of the vehicle model – considering algorithm 4Points – are presented in Figure 21(a). Two phases of motion can be differentiated here when first front wheels and then rear wheels of the vehicle drive over the bump.

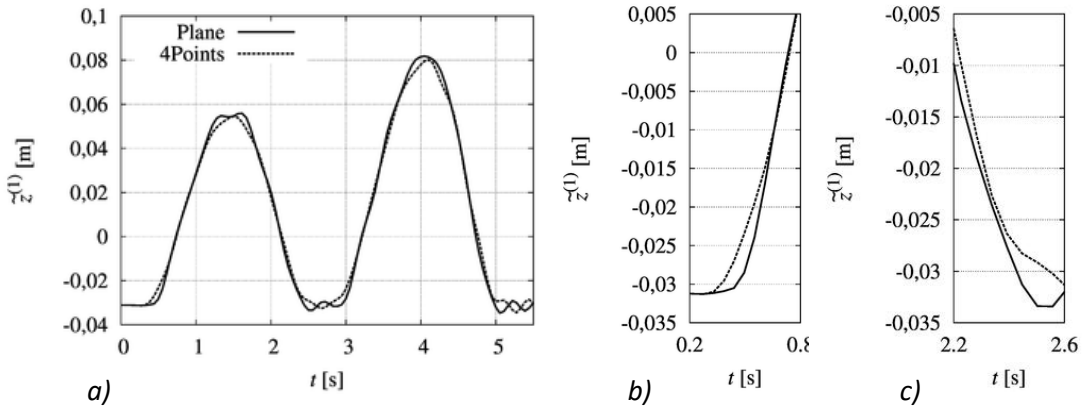

Figure 21. A course of the vertical displacement of the vehicle gravity center when the discrete model of the road surface made by use of rectangles is considered

By analyzing the results in Figure 21(a), it can be noticed that when the 4Points algorithm is used, the displacement of the gravity center of the vehicle while its going up to the bump, takes place earlier than in the case of the Plane algorithm – the dashed line is visible before the solid line (Figure 21(b)). The analogical situation can be observed during the vehicle going down from the bump. In this case the 4Points algorithm is more „sensitive" to the unevenness profile change behind the wheels – the dashed line is visible behind the solid line (Figure 21(c)). Therefore, the thesis is confirmed that in the case of overcoming unevenness, where the road fragments are flat, better results are obtained when the 4Points algorithm is used.

Within realization of the doctoral dissertation [10] a number of test computer simulations, verifying effectiveness of the presented algorithms with reference to the assumed models of the road surface, were made. The computer results were verified positively after comparing them to the experimental test results made on the test track.

9 CONCLUSIONS

The presented algorithms have a general significance and that is why they can be used in future in the case of considering more advanced tire models. In order to sum up this article it should be emphasized that the development of the presented algorithms was only a part of the task undertaken by the authors. These algorithms with the tire models were included into the advanced mathematical model of the selected terrain vehicle, developed with view to performing an analysis of its dynamics. This model with the prepared models of the road surface and the developed computer programs constitute a prototype of a technical rescue vehicle. According to the authors, the observations made during the computer simulations of its motion can aid a process of designing of this type of vehicles in the future. In addition to the statements presented, the authors would like to point out to wide use – in the case of the proposed method – of possibilities of the Blender program, especially while developing the road surface models, and also a vehicle model used in the computer animations.

REFERENCES

[1] Craig J.J., Introduction to Robotics. Mechanics and Control, Addison-Wesley Publishing Company, Inc, 1989, 1986

[2] Grzegożek W., Adamiec-Wójcik I. and Wojciech S. Computer Modelling of dynamics of motor vehicles (in Polish), Publisher of Technical University of Cracow, Cracow 2003.

[3] Hirschberg W., Rill G., Weinfurter H., Tire model TMeasy, Vehicle System Dynamics, Vol.45, 2007, pp.101-119

[4] Hirschberg W., Rill G., Weinfurter H., User-Appropriate Tyre-Modeling for Vehicle Dynamics in Standard and Limit Situation, Vehicle System Dynamics, Vol.38, No.2. 2002

[5] Keys R., Cubic convolution interpolation for digital image processing, Acoustics, Speech and Signal Processing, Vol. 29, pp. 1153-1160, 1981

[6] Pacejka H.B, Bakker E., Lidner L., New Tire Model with an Application in Vehicle Dynamics Studies, SAE Technical Paper 890087, 1989

[7] Pacejka H.B., Bakker E., The Magic Formula Tyre Model, Vehicle System Dynamics, Vol.21, 1993, pp. 1-18

[8] Pacejka H.B., Spin: camber and turning, Vehicle System Dynamics, Vol.43, 2005, pp.3-17

[9] Rill G., TMeasy – The Handling Tire Model for all Driving Situations, in: Savi M.A. (ed.), Proc. of the XV International Symposium on Dynamic Problems of Mechanics DINAME 2013, Buzios, Brazil, 2013

[10] Tengler S., Analysis of dynamics of special vehicles with high gravity center (in Polish), PhD Thesis, Faculty of Mechanical Engineerim and Computer Science, University of Bielsko-Biala, Poland, 2012
[11] Unrau H.-J., Zamow J., TYDEX-Format. Description and Reference Manual. Release 1.3, 1997
[12] www.blender.org